Toughening of a Trifunctional Epoxy System. II. Thermal Characterization of Epoxy/Amine Cure

R. J. VARLEY,[1] J. H. HODGKIN,[1] D. G. HAWTHORNE,[1] and G. P. SIMON[2,*]

[1]CSIRO Division of Chemicals and Polymers, Bayview Avenue, Clayton, Victoria 3168, and [2]Department of Materials Engineering, Monash University, Wellington Road, Clayton, Victoria 3168, Australia

SYNOPSIS

The cure of a trifunctional epoxy resin with an amine coreactant was studied using two thermal analysis techniques: differential scanning calorimetry (DSC) and dynamic mechanical thermal analysis (DMTA). These techniques were used to monitor the development of both the thermal and mechanical properties with cure. Detailed kinetic analysis was performed using a variety of kinetic models: *n*th order, autocatalytic, and diffusion-controlled. The reaction was found to be autocatalytic in nature during the early stages of cure while becoming diffusion-controlled once vitrification had taken place. By combining the results obtained from DSC and DMTA, the degree of conversion, at which key events such as gelation and vitrification take place, were determined. A TTT diagram was constructed for this epoxy/amine system showing the final properties that can be achieved with the appropriate cure history. © 1996 John Wiley & Sons, Inc.

INTRODUCTION

High-temperature epoxy resin composite systems continue to be widely used as structural materials in the aerospace industry due to their favorable mechanical properties such as high modulus and thermal stability, coupled with low shrinkage on curing. Nonetheless, considerable research is continuing on strategies for toughening these inherently brittle materials. This work has generally focused on the incorporation of a second component within the epoxy matrix. In general, the toughening additive is initially soluble in the uncured epoxy/amine mixture, precipitating out as the material polymerizes. Rubber, rigid filler particles and thermoplastics have been used widely for this purpose and a summary of some of the systems investigated and mechanisms of toughening have been detailed elsewhere.[1] Use of thermoplastics as effective toughening agents would generally be the desirable option since, unlike the inclusion of rubber, addition of thermoplastics does not lead to significant reductions in modulus and heat-distortion temperatures. To date, most research on thermoplastic toughening has concentrated on bifunctional[2-4] and tetrafunctional[5,6] epoxy systems. However, a number of advanced composite prepregs contain a significant proportion of the trifunctional epoxy material known as trisglycidyl-*p*-aminophenol (TGAP) in combination with tetrafunctional tetraglycidyl diaminodiphenylmethane (TGDDM).[7] In addition, TGAP is being used in high-temperature adhesives,[8] although, currently, its properties are often inadequate. The use of such trifunctional epoxy materials, rather than tetrafunctional epoxies, is potentially desirable,[9] since the lower crosslink density and modulus may be offset by increased toughness when compared to TGDDM-based systems.

To date, studies of the thermoplastic toughening of trifunctional resin systems have demonstrated only moderate improvement in toughness[10-13] and this may be due, in part, to an incomplete understanding of the effect the structure and reactivity of the thermoplastic has on the cure, morphology, and fracture toughness. Other studies, e.g., with bifunctional epoxy monomers, show that the use of phenolic hydroxyl or aromatic amine end groups on the thermoplastic significantly improved fracture toughness.[14] More recent work has described other

* To whom correspondence should be addressed.

Journal of Applied Polymer Science, Vol. 60, 2251–2263 (1996)
 CCC 0021-8995/96/122251-13

aspects of TGAP/thermoplastic blend systems[15,16] and is indicative of a continuing interest in this combination of materials.

The use of functionalized poly(ether sulfone) thermoplastic in a trifunctional TGAP system is being investigated in detail in our laboratory. As part of this systematic study, the first article of the series[17] examined the kinetics of the cure of TGAP/DDS by near-infrared spectroscopy (NIR). In the current article, the results of thermal cure monitoring of the neat resin system are presented to better understand the mechanism of the cure process. This process, in turn, helps to control the final morphology, both of the neat resin and the thermoplastic-dispersed blend, necessary in order to optimize fracture toughness. Despite its widespread commercial use, there are, to our knowledge, no reliable curing studies of TGAP using thermal analysis techniques or the subsequent application of data arising from those techniques to various kinetic models.

EXPERIMENTAL

Materials

TGAP (Ciba-Geigy, MY0510) and an aromatic amine hardener, 4,4′-diaminodiphenyl sulfone (DDS, Ciba-Geigy, HT976) were used without further purification. Materials were characterized by HPLC techniques and the epoxy equivalent weight of the TGAP monomer was determined by titration to be 9.41 mmol/g.

Sample Preparation

The resin mixture of catalyzed epoxy monomer was prepared by adding 52 wt % DDS (corresponding to a 1 : 0.9 epoxy-to-amine molar ratio) to the TGAP resin at 130°C and mixing until the solution became clear. The clear melt was degassed until no bubbles remained. A slight excess of epoxy is generally used in this type of resin system,[18] because if an epoxy/amine ratio of 1 : 1 is used, many of the remaining amine functional groups fail to react following spatial entrapment in an immobile, rigid epoxy network.[17] Excess amine in a cured composite serves only to further aid moisture ingress and decrease mechanical properties of the polymer.[19,20]

Instrumental Techniques

Two thermal analysis methods, differential scanning calorimetry (DSC) and dynamic mechanical thermal analysis (DMTA), were used to investigate the thermoset polymerization process. A combination of both isothermal and dynamic scan techniques were carried out.

Differential Scanning Calorimetry

DSC experiments were carried out using a Mettler 400TA machine which was calibrated using indium. The samples were placed in aluminum sample pans and experiments were performed under a flow of dry nitrogen gas. Temperature scan experiments were performed at 2, 5, 10, 20, and 30°C/min while most isothermal experiments were done from 100 to 220°C at 10°C intervals. After the isothermal cure, the polymer was subjected to a dynamic scan from 50 to 300°C at 10°C/min.

Dynamic Mechanical Analysis

Mechanical analysis was performed on a Polymer Laboratories DMTA fitted with a Mark II power head. To follow the cure process from the liquid monomer to the rigid thermoset stage, it was necessary to support the material on an inert substrate such as a braid.[21] Glass fiber tape was impregnated with the resin, which was then secured into a 5 mm free length frame using knife-edged clamps. For isothermal experiments, the temperature was ramped up at a rate of 25°C/min to just below the desired temperature. The samples were cured to completion isothermally over a range of temperatures from 100 to 180°C in 10°C steps. Once the material had cooled down after cure, the resultant polymer was scanned from 50 to 300°C at a rate of 2°C/min.

RESULTS AND DISCUSSION

Differential Scanning Calorimetry

The heat of reaction (ΔH) of the epoxy/amine cure was found to be 684.0 J/g as determined from the average of the dynamic scans and this was used in future calculations as the total heat of reaction, Q_0.[22] This Q_0 amounts to 110.5 kJ/mol of epoxide, in agreement with the literature which reports that most epoxy/amine values lie between 103 and 110 kJ/mol.[23]

Dynamic Scans

An average activation energy, E_a, can be determined using the Kissinger equation[24]:

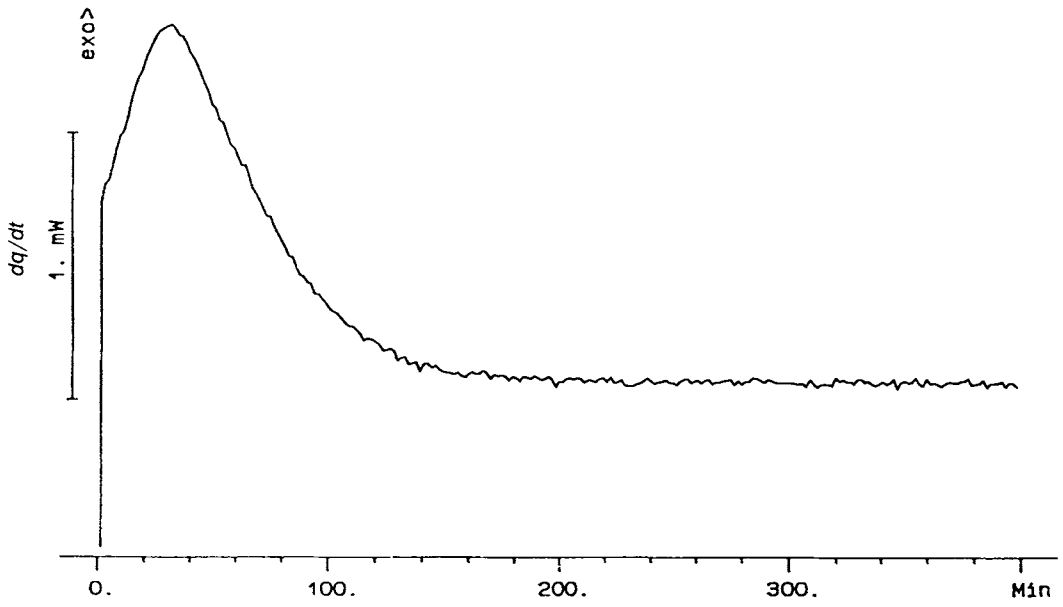

Figure 1 Typical DSC thermogram of TGAP/DDS cured isothermally at 150°C.

$$-\ln(\phi/T_p^2) = \frac{E}{RT} - \ln(AR/E_a) \qquad (1)$$

where ϕ is the heating rate; T_p, the peak exothermic temperature; A, the frequency (pre-exponential) factor; and R, the gas constant. This results in a value of 50.9 kJ/mol and compares well with an E_a of 55.4 kJ/mol[25] reported elsewhere for the TGAP/DDS system. Determination of activation energy and polymerization kinetics from temperature scanning DSC experiments (either multiple scan as above or single scan[26]) is fraught with difficulties. Not only is there the experimental limitation of the thermal lag experienced by the sample as the temperature is scanned, but the use of an equation such as the Kissinger equation also makes a number of theoretical assumptions, the main being that the reaction mechanism consists of one predominant reaction step (in this case, epoxy/amine addition) and ignores other possibilities such as polyetherification[27-29] which can occur under certain conditions. The wide range of temperatures that are often scanned to produce a "complete" exotherm with a flat base line on the low- and high-temperature sides may induce additional events. For example, the possibility of thermal degradation and thus slight plasticization of the system is possible on the higher-temperature side of the scan.

Isothermal Scans

Due to the experimental difficulties associated with dynamic DSC, the detailed kinetic studies were performed using isothermal DSC only. A typical isothermal DSC thermogram is shown in Figure 1. It quite clearly shows the rapid increase in the heat output followed by an exponential decrease with time ending in a flat line. The data as recorded by the DSC is dq/dt, where q is the thermal energy flow (in the case of curing systems and q is exothermic). Thus, by integrating the area under the exotherm, it is possible to determine the partial peak area, Q_t, as a function of time.[30] The degree of thermal conversion, α, at any time t is thus

$$\alpha = \frac{Q_t}{Q_0} \qquad (2)$$

The α vs. time plots for TGAP/DDS over a range cure temperatures are shown in Figure 2. It can be seen that the rate of conversion increases with increasing temperature, as does the ultimate level of conversion. Curing for long times at 100°C leads to a final thermal conversion of about $\alpha = 0.64$, whereas cure at 220°C leads to an essentially total thermal conversion ($\alpha = 0.99$); these data are shown in Table I. Also presented is the time at which the exothermic

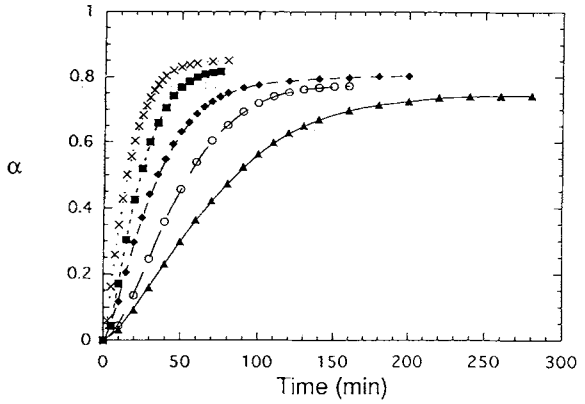

Figure 2 Degree of conversion, α as a function of time at a range of temperatures: (▲) 140°C; (○) 150°C; (♦) 160°C; (■) 170°C; (×) 180°C, as determined by isothermal DSC kinetics.

peak has a maximum value for a given isothermal cure, t_p^{iso}. This will be compared later with other key events in the cure such as gelation and vitrification.

The glass transition temperature of the final material can also be obtained by rescanning the cured samples. A typical DSC thermogram as shown in Figure 3 highlights the endothermic variation due to the T_g, followed by the resultant residual exotherm. It can be seen that the T_g of 200°C was somewhat greater than the isothermal cure temperature (150°C); the reasons for this will be discussed later.

From the conversion vs. time plots that have been constructed, kinetic analysis was performed by fitting the curves to a power of six polynomial, so that the derivative, $d\alpha/dt$, could be calculated from a simple computer program. The resulting coefficients obtained from the curve fit of the polynomial were then analyzed using this program to give the kinetic information required.

General Kinetics

The simplest equation able to fit the isothermal data is[30]

$$r = \frac{d\alpha}{dt} = kf(\alpha) \tag{3}$$

where r is the rate of the reaction; k, the apparent reaction rate; and $f(\alpha)$, some functional dependence of rate on conversion, $\alpha(t)$. If the apparent rate constant is of the form

$$k = A \exp\left(\frac{-E_a}{RT}\right) \tag{4}$$

where A is the preexponential factor; E_a, the apparent activation energy; and R, the gas constant, then

$$\ln r = \ln A - E_a/RT + \ln[f(\alpha)] \tag{5}$$

Thus, if ln r is determined experimentally and plotted against $1/T$ for a given conversion, E_a can be determined for that degree of reaction. The range of isothermal data measured is shown in Figure 4 for degrees of cure α = 0.1–0.9 and is also summarized in Table II. The linearity of the dependencies in Figure 4 indicate that despite the simplicity of the model it does provide a good fit to the kinetics of TGAP cure at various conversions. Also included in Table II for comparison is similar data for two other well-known di- and tetrafunctional epoxy systems cured with DDS, the diglycidyl ether of bisphenol-A (DGEBA),[31] and tetra-*N*-glycidyl-4,4′-diaminodiphenyl methane (TGDDM),[32] respectively.

These data are also shown graphically in Figure 5 for the three systems and a number of noticeable factors are apparent. First, the activation energies are all of similar value ranges with the trifunctional TGAP being lowest at low conversions. Second, the activation energies of both TGAP and TGDDM increased dramatically as a function of conversion, while the lower crosslinked density DGEBA stayed

Table I Comparison of Isothermal Kinetic DSC Experiments for TGAP at a Range of Cure Temperatures

Cure Temperature	Ultimate Conversion	t_p^{iso} (min)	T_g (°C)
100	0.64	616.0	133.00
110	0.67	470.2	138.00
120	0.70	97.2	157.00
130	0.72	92.8	172.00
140	0.74	36.0	191.00
150	0.77	32.0	199.00
160	0.80	14.4	208.00
170	0.82	12.8	[a]
180	0.85	6.0	[a]
190	0.89	5.5	[a]
200	0.92	4.0	[a]
210	0.97	2.8	[a]
220	0.99	2.0	[a]

The parameters shown are the ultimate conversion at long cure times, the time for maximum heat evolution from the DSC thermogram, t_p^{iso}, and the T_g from dynamic DSC scanned at 10°C/min.

[a] Glass transition not observed in the dynamic scan.

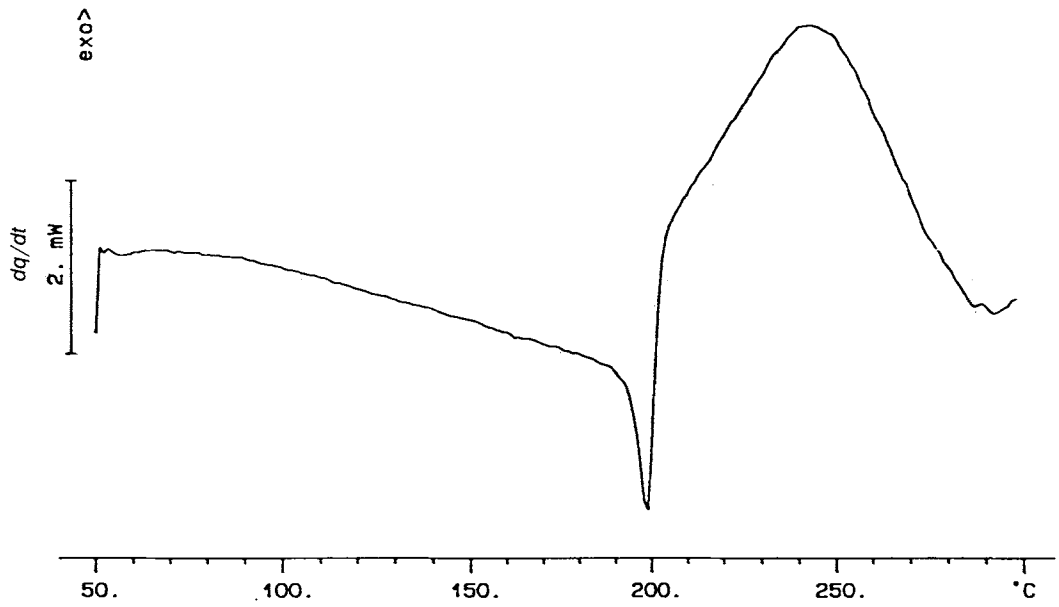

Figure 3 Typical DSC thermogram of a dynamic rescan after isothermal cure of TGAP/DDS at 150°C.

approximately constant. Third, the variation of E_a with cure in the more highly crosslinked systems indicates that the reaction is complex and that diffusional processes become increasingly important.[32]

As indicated by this model, higher functionality, i.e., tri- and tetrafunctional epoxies, results in greater activation energies at high degrees of conversion as the epoxide unit motion becomes inhibited in the matrix. Stutz and Mertes[23] also demonstrated recently that the chemical nature of the polymer network affects activation energy and that the *O*-epoxypropyl groups found in DGEBA have a lower energy of activation compared to the energy of activation of the *N*-epoxypropyl groups in the unreacted TGDDM and TGAP molecules attached to the network. Figure 5 illustrates that the increase in activation energy occurs rapidly after conversions of 0.6 for TGAP and rather more gradually for TGDDM at all conversions, although in the latter case, the increase is more dramatic above conversions of 0.6.

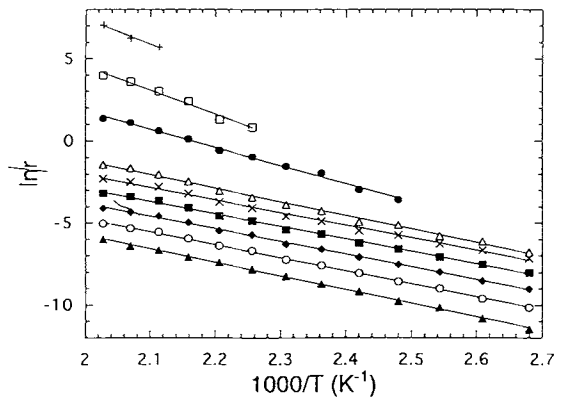

Figure 4 Natural log of the reaction rate (ln r) vs. reciprocal temperature ($1/T$) for a range of conversions (α): (▲) 0.1; (○) 0.2; (♦) 0.3; (■) 0.4; (×) 0.5; (△) 0.6; (●) 0.7; (□) 0.8; (+) 0.9.

Table II Comparison of Difunctional (DGEBA),[31] Trifunctional (TGAP), and Tetrafunctional (TGDDM)[32] Apparent Activation Energies as a Function of Conversion (a) Using Eq. (5)

	E (kJ/mol)		
α	DGEBA	TGAP	TGDDM
0.1	84.5	69.0	68.0
0.2	78.5	65.8	69.0
0.3	75.6	64.2	70.0
0.4	73.8	63.4	72.0
0.5	73.3	64.0	75.0
0.6	71.4	69.3	81.0
0.7	70.8	91.4	88.0
0.8	69.9	121.3	99.0
0.9	69.2	127.9	155.0

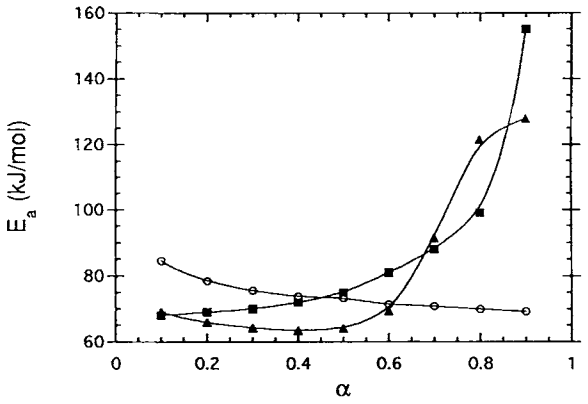

Figure 5 Activation energy (E_a) vs. conversion (α) for three systems: (○) DGEBA, Ref. 31; (▲) TGAP (this article); (■) TGDDM, Ref. 32.

*n*th-Order Kinetics

An improvement to eq. (3) often involves the assumption of "*n*th-order" kinetics where $f(\alpha)$ is described as

$$f(\alpha) = (1 - \alpha)^n \tag{6}$$

and leads to the equation analogous to eq. (5):

$$\ln r = \ln k + n \ln(1 - \alpha) \tag{7}$$

A plot of $\ln(1 - \alpha)$ vs. $\ln r$ would be linear if the reaction obeyed *n*th order kinetics and would be a maximum at $t = 0$. Figure 6 illustrates the relationship for two cure temperatures when applied to the TGAP/DDS system—note that $\ln(1 - \alpha) = 0$ represents a degree of conversion of $\alpha = 0$. It can be seen that $\ln(1 - \alpha)$ vs. $\ln r$ is far from linear and that the maximum rate is not at $t = 0$ but between $\alpha = 0.2$ and 0.4 [$\ln(1 - \alpha)$ between -0.2 and -0.5]. This indicates that the reaction is autocatalytic with diffusion control occurring at higher conversions. Clearly, as in other systems,[31,33] *n*th-order kinetics does not fully describe the reacting TGAP system.

Autocatalytic Kinetics

Horie et al.[34] derived kinetic equations which took into account autocatalysis early in the reaction (due to increased hydroxyl concentration from primary amine/epoxide reaction) with the resultant rate equation being of the form

$$r = (k_1 + k_2\alpha^m)(1 - \alpha)^n \tag{8}$$

where k_1 and k_2 are temperature-dependent rate constants, as are exponents m and n. It is often found that $m = 1$ and $n = 1$ if the rate-determining step is a bimolecular interaction between an hydroxyl group and either an amine group or an amine-epoxide species.[30,35] If $m = 1$ and $n = 2$, it has been suggested that the rate-determining step is a termolecular reaction among hydroxyl, amine, and epoxide groups.[34,36] Some workers have assumed that $m + n = 2$ when fitting eq. 8,[37-40] usually leading approximately to $m = n = 1$.

Often it is assumed that $m = 1$ and, thus, a plot of α vs. $r/(1 - \alpha)^n$ should be a straight line for a fitted value of n. It is easier to choose an appropriate value of n by comparing the experimental rate of reaction with that determined by fitting n, k_1, and k_2 to eq. (8). For our work, this was done for all cure temperatures and an example is shown in Figure 7 for a 150°C cure for $n = 1$, 2, and 3 and the experimental reaction rate is also plotted. Viewing data for all cure temperatures (not all shown here) indicated that the best overall fit was for $m = 1$ and $n = 2$. Clearly, even the fit for $n = 2$ is far from perfect and overestimates the cure rate at low and high conversions. This is true in other systems such as reported by Sourour and Kamal,[41] where the fit was best between 40 and 60% conversion. Poor fits at low conversion could indicate a rather more complex mechanism for autocatalysis than the bimolecular or termolecular ones proposed. Barton[22,26] suggested that ether-forming reactions such as homopolymerization or epoxide/hydroxyl reactions are not accounted for in these models and these may also be important. However, etherification has been shown not to be a problem at low conversions, usually becoming dominant near and beyond vitrification.[15,17,42,43]

The values of and k_1 and k_2 for $m = 1$ and $n = 2$ for a range of cure temperatures for the TGAP sys-

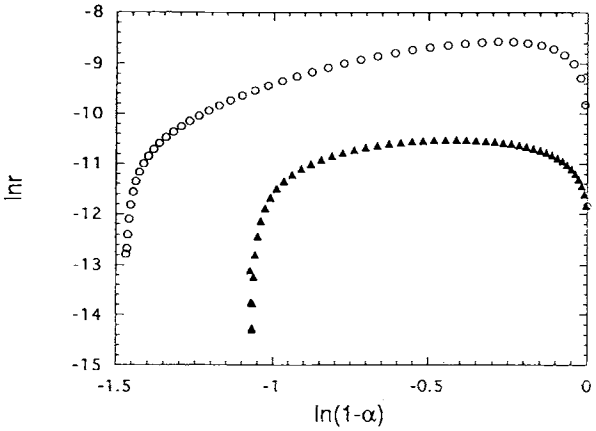

Figure 6 Plot of $\ln r$ vs. $\ln(1 - \alpha)$ for TGAP isothermal DSC cure at temperatures: (▲) 150°C; (○) 110°C.

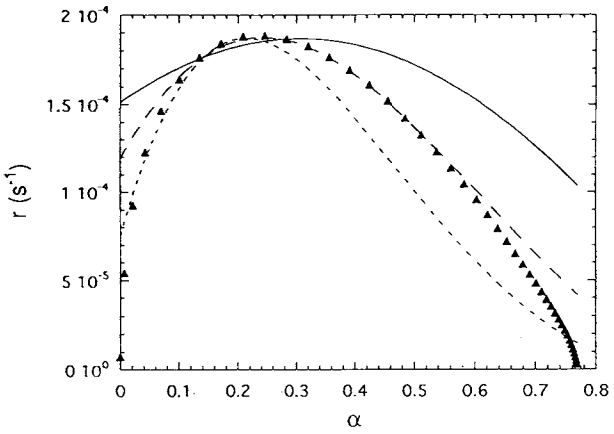

Figure 7 Fitting of autocatalytic eq. (8) to experimental rate data (r) at 150°C isothermal cure. Experimental rate data given by (▲). In all cases, the fits use (——) $m = 1$ and $n = 1$, (— — — —) $n = 2$, and (– – – – –) $n = 3$.

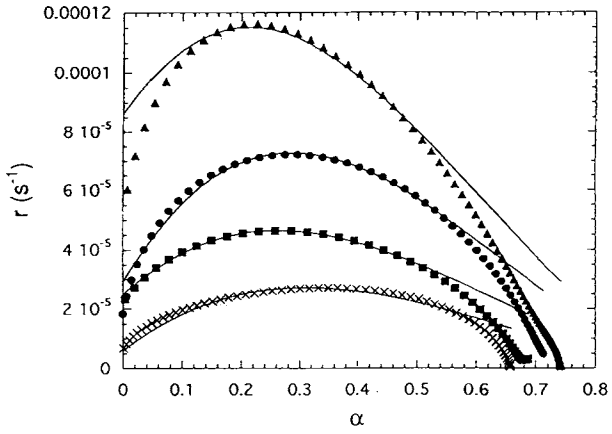

Figure 8 Fitting of autocatalytic eq. (8) to experimental rate data (r) for $m = 1$ and $n = 2$ for various temperatures. Experimental data is (×) 110°C, (■) 120°C, (●) 130°C, and (▲) 140°C. The solid line is the theoretical fit in each case.

tem are given in the first three columns of Table III. As expected, the rates increase with temperature. Figure 8 shows fits for $n = 2$ and $m = 1$ for a range of temperatures. The goodness of fit varies with cure temperature. This is similar to work done by Cole et al.[43] who examined epoxy prepregs consisting largely of TGDDM and DDS and found that the ability to fit eq. (8) adequately, varied with temperature, as did values of n and m, indicating the potential limitations of eq. (8). A very recent paper by Kenny[44] described a method of determining m and n directly without the need to set m or $m + n$ at a particular value. In that work, a high-temperature dicyanate resin yielded a value of $m = 0.98$ and $n = 1.12$.

Diffusion-control Kinetics

The often-observed poor fit at high conversions[30] is ascribed to diffusion control of the reaction. This would be expected at high conversions as the network T_g approaches the cure temperature and is coincident with the likelihood of the reaction becoming increasingly localized through spatially separated entrapment of reactive groups.

Table III Kinetic Parameters Obtained from Fitting Autocatalytic Kinetics Eq. (8) and Autocatalytic Kinetics and Diffusion Control Eq. (9)

Isothermal Cure Temperature (°C)	Autocatalytic Kinetics $m = 1, n = 2$		Autocatalytic Kinetics and Diffusion Control $m = 1, n = 1$			
	$k_1 \times 10^{-4}$ (s^{-1})	$k_2 \times 10^{-4}$ (s^{-1})	$k_1 \times 10^{-4}$ (s^{-1})	$k_2 \times 10^{-4}$ (s^{-1})	$s_1 \times 10^{-4}$ (s^{-1})	$s_2 \times 10^{-4}$ (s^{-1})
100	0.048	0.727	0.035	0.978	0.033	0.928
110	0.060	1.649	0.071	1.716	0.075	1.831
120	0.248	2.321	0.137	3.770	0.189	5.219
130	0.290	4.004	0.154	5.720	0.198	7.342
140	0.860	4.727	0.486	8.030	0.636	10.503
150	1.190	8.624	0.562	12.625	0.670	15.071
160	1.923	10.933	1.723	15.820	2.105	19.330
170	3.082	19.359	2.388	23.359	2.621	25.641
180	4.475	24.959	4.775	26.214	4.961	27.240
Activation energy (kJ/mol)	79.6	62.0	85.6	58.3	86.2	58.9

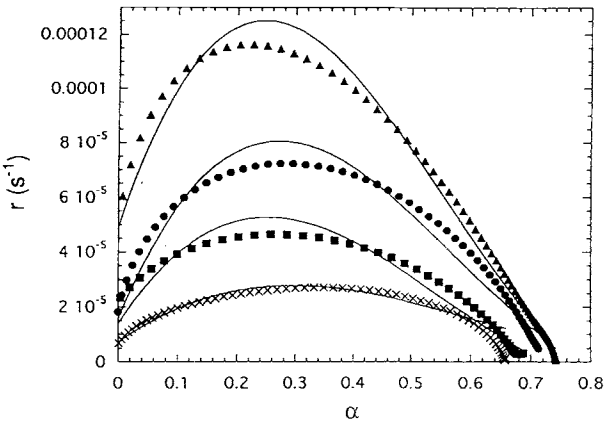

Figure 9 Fitting of autocatalytic and diffusion control eq. (9) for experimental rate data for $m = 1$ and $n = 1$ for various temperatures of cure: (×) 110°C; (■) 120°C; (●) 130°C; (▲) 140°C. The solid line is the theoretical fit in each case.

Two methods of taking account of this latter phenomenon will be examined in the TGAP system. If it is assumed that k_1 and k_2 from eq. (8) decrease linearly with conversion,[22] the modified rate constants $k_i = k_i - s_i\alpha$ for $i = 1$ and 2 can be defined, which leads to the relationship

$$r = (A_0 + A_1\alpha + A_2\alpha^2)(1 - \alpha)^n \qquad (9)$$

if $m = 1$. In eq. (9), $A_0 = k_1$, $A_1 = k_2 - s_1$, and $A_2 = -s_2$. As with eq. (8), best fits were obtained and compared with experimental reaction rates for $m = 1$ and $n = 1$, 2, or 3. It was found that $n = 1$ produced the best fit for all cure temperatures. Curve fits of experimental data $m = n = 1$ are shown in Figure 9.

Table III shows the values of k_1, k_2, s_1, and s_2 for the range of cure temperatures. Even though $n = 1$ was ultimately used as the exponent in eq. (9), compared to $n = 2$ in eq. (8), values of k_1 and k_2 were relatively similar. The goodness of fit as seen in Figure 9 (compared to Fig. 8) is slightly improved (with a good fit being achieved in curves up to $\alpha = 0.7$ depending on temperature. The fit is still not good at very high conversions, suggesting that diffusion control is responsible for a greater than linear decrease of k_1 and k_2 with conversion. Barton[22] who demonstrated the applicability of this equation previously did so with a difunctional epoxy system and a lower crosslink density. Clearly, the higher crosslink density of TGAP shows a greater decrease in reaction rate with conversion. The values of k_1, k_2, s_1, and s_2 are shown (along with their activation energies) in Table III. The values are similar to those reported elsewhere.[40,43]

An alternative approach to diffusion-control modeling is that of Chern and Poehlein[45] who proposed a WLF-type function (which models the change in polymer properties based on variation in free volume). It can be combined with autocatalysis [eq. (8)] to model changes in the reaction rate.[45] This involves determination of $f(\alpha)$, which represents diffusion control, where

$$r = (k_1 + k_2\alpha^m)(1 - \alpha)^n f(\alpha) \qquad (10)$$

where

$$f(\alpha) = \frac{1}{1 + \exp[C(\alpha - \alpha_c)]} \qquad (11)$$

in which C and α_c are curve-fitted variables. The function $f(\alpha) = 1$ for small values of conversion and decreases at high conversions. $f(\alpha)$ is calculated and fitted by dividing experimental rate r in eq. (10) by the autocatalytic term with the best-fit values of k_1, k_2, m, and n at lower conversions already determined (see Table III). α_c is the critical conversion at which diffusion starts to dominate the kinetics.

It is of interest to follow the function $f(\alpha)$ as a function of cure for a range of cure temperatures and this is shown in Figure 10. It can be seen that at conversions of greater than $\alpha = 0.55$ (well above gelation) the function $f(\alpha)$ (which describes the decreasing mobility of reactive units, based on inhibited reaction kinetics, due to the loss of free volume and molecular mobility) is dependent on conversion and the cure temperature. Figure 11 shows that with increasing temperature the conversion at which dif-

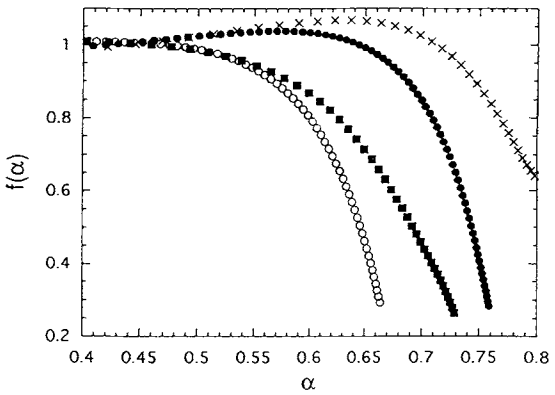

Figure 10 Plot of $f(\alpha)$ vs. α [from eq. (11)] for a range of cure temperatures: (○) 120°C; (■) 140°C; (●) 160°C; (×) 180°C.

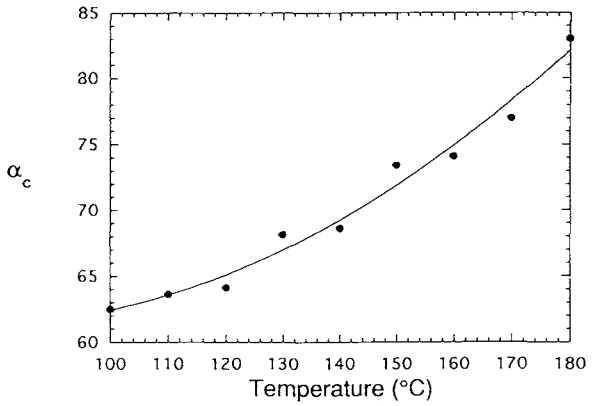

Figure 11 Plot of α_c (●) from eqs. (10) and (11) as a function of cure temperature.

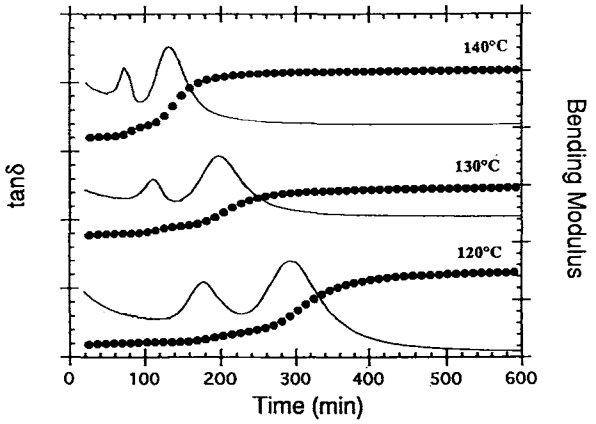

Figure 12 (——) Sample isothermal DMTA cure of mechanical loss (tan δ) and (●) bending modulus as function of time for a range of cure temperatures.

fusion-control kinetics begins to dominate occurs at a higher and higher conversion. This is due to the resin being able to stay mobile longer at the higher temperatures. Cole et al.,[43] using a similar model, also found that the downturn in $f(\alpha)$ at α_c occurred at increasingly higher conversions for higher cure temperatures—essentially at the point at which the epoxy–amine reaction is complete and the epoxy etherification reaction becomes significant. Khanna and Chanda[33] found, generally, in a stoichiometric DGEBA/anhydride-cured system that α_c increased with temperature, although, surprisingly, at low levels of the catalyst, it was largely independent of temperature.

Clearly, the models used in this work have limitations. However, their relative simplicity and the ability to obtain rate and conversion parameters (k_1, k_2, α_c, etc.) make them useful in the modeling of thermoset systems. While other models that have been developed often to take into account etherification,[30,46] these usually require assumptions about reaction rates, enthalpies, and the nature of the catalytic complexes formed. To aid in the understanding and modeling of the TGAP system, DSC thermal analysis is now linked to the *in situ* dynamic mechanic analysis presented in the next section.

Dynamic Mechanical Analysis (DMA)

The use of DMA to monitor the change in the physical state of crosslinking systems was developed by Gillham over a long period of time.[21] As a viscoelastic cure monitoring technique, it has the advantage over techniques such as rheometry in that it can monitor critical events such as both gelation and vitrification, whereas rheometry is only able to monitor gelation. Typical isothermal DMA curves can be seen for TGAP specimens for a range of cure temperatures with both modulus and mechanical loss (tan δ) displayed in Figure 12. There are two peaks in the tan δ trace—the first associated with gelation and the second with vitrification. As expected, these events occur at shorter times with increased cure temperature. Also shown in Figure 12 is the increase in modulus as a function of cure, eventually plateauing out beyond vitrification, indicating that no further reaction is occurring.

Figure 13 describes the degree of conversion of key events in the TGAP cure as a function of cure temperature. In addition to gelation and vitrification (tan δ maxima), conversion at an "infinitely long" isothermal cure, the point at which DMA modulus begins to plateau, and the conversion at which isothermal DSC thermogram shows a maxima are also

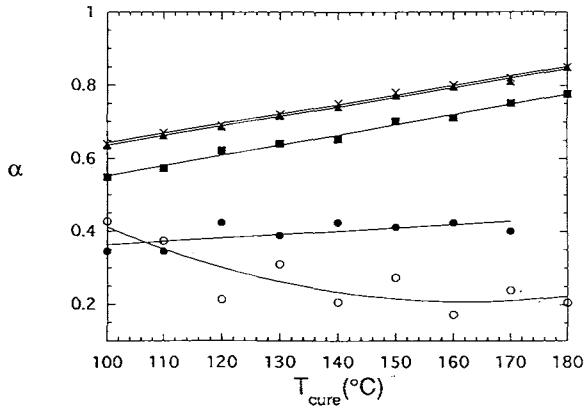

Figure 13 Isothermal cure temperature (T_{cure}) vs. conversion for key events. The various events are (○) DSC maximum), (●) gelation, (■) vitrification, (▲) beginning of modulus plateau, and (×) after "infinite" cure time.

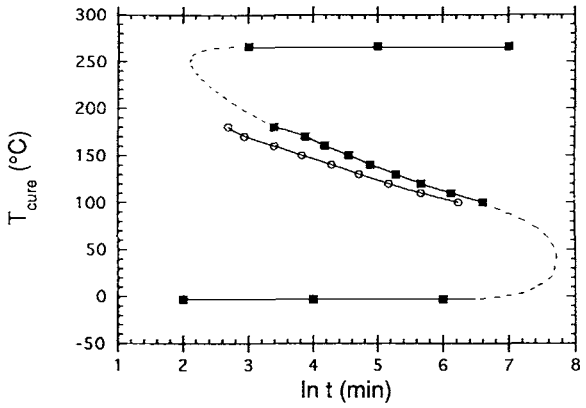

Figure 14 Time–temperature–transformation (TTT) diagram of TGAP/DDS showing (○) gelation and (■) vitrification.

included. It can be seen from Figure 13 that conversion at gelation is reasonably constant with the cure temperature (between $\alpha = 0.35$ and 0.42). The calculation of gel conversion by Flory[47] assumed that gel conversion was independent of the cure temperature and should equal p_{gel}, where

$$p_{gel}^2 = \frac{1}{(f-1)(g-1)} \tag{12}$$

in which f and g are the functionality of the TGAP ($f = 2$) and DDS ($g = 4$). This yields a $p_{gel} = 0.4$ which (perhaps fortuitously) lies within the range of experimentally measured conversions. Factors such as cyclization and side reactions generally tend to result in gelation conversions greater than that expected from eq. (12). It can be seen that vitrification, the point of the modulus plateau, and the "infinitely long" cured sample all show an increased degree of cure with higher cure temperatures, as expected.

From an Arrenhius-like plot of $1/T_{cure}$ vs. log t_{gel}, an energy of activation of 62 kJ/mol was calculated. Interestingly, this is very close to the activation energy of reaction determined from DSC using eq. (5) prior to vitrification, as seen in Table II. The correlation between DSC and DMTA analysis validates the assignment of the gelation peak in the DMTA spectra. It indicates that the energy barriers that must be overcome to result in reaction (DSC) measurements are similar to those involved in the molecular mobility (DMTA) measurements. The plot of $1/T_{cure}$ vs. log time for vitrification is not linear due to the conversion at vitrification being dependent on cure temperature, thus preventing an activation energy barrier being measured.[48]

From the gelation and vitrification times obtained, a time–temperature–transformation (TTT) diagram has been constructed as shown in Figure 14. This phase diagram allows the prediction of physical states through a range of cure profiles. The characteristic shape of the vitrification curve for the DGEBA/DDS[49] cure is not nearly as evident for the TGAP/DDS system, with vitrification always occurring soon after gelation regardless of temperature. The vitrification peak remains strong and sharp at all temperatures unlike for DGEBA-based systems. This is believed to be due to the higher functionality of TGAP having more reactive sites in close proximity to each other in the gelled state as opposed to a bifunctional DGEBA/DDS system with fewer reactive sites available.

The glass transition temperature was also followed as a function of cure time. The material was cured to the peak reaction rate (as determined from DSC), to gelation, to vitrification, to the end of the modulus increase, and to completion. The material was then cooled and the T_g determined from a DMTA rescan. The change in the T_g's are displayed for the various cure temperatures (Fig. 15). After a rapid increase, the rise in the T_g begins to slow down until it reaches a plateau after which no further increase is observed. The lack of an apparent plateau in the T_g for the 160 and 180°C cures is due to a gradual decrease in the intensity of the tan δ peak until no glass transition peak is observed. This phenomenon is discussed later in the text.

Figure 16 shows the T_g^∞ (T_g at infinitely long cure times for a given cure temperature) for both the DSC and DMTA plotted as a function of cure temperature. It could be expected from theory that the reaction would cease when $T_g = T_{cure}$ (Ref. 21) and,

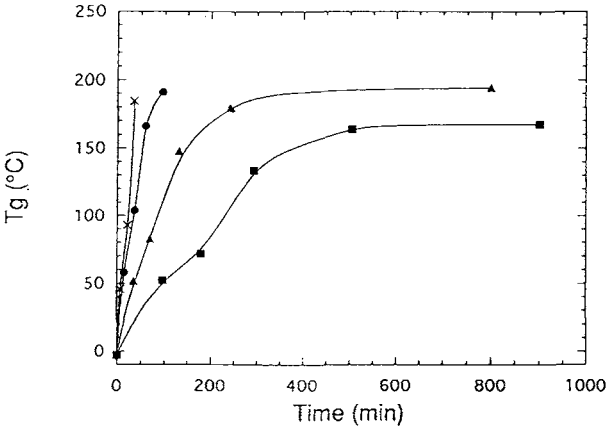

Figure 15 T_g as a function of isothermal cure time as measured by DMTA for various cure temperatures: (×) 180°C; (●) 160°C; (▲) 140°C; (■) 120°C.

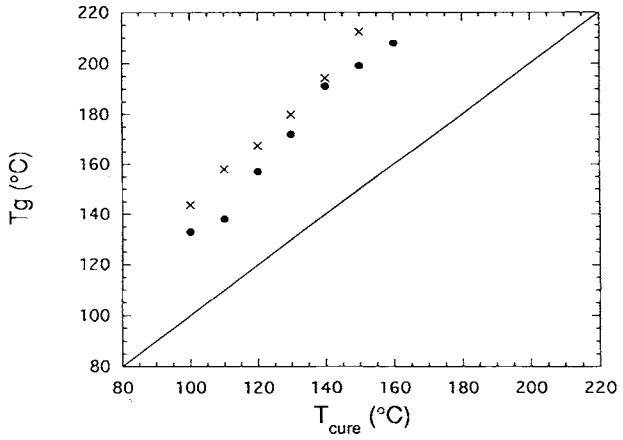

Figure 16 T_g as measured by (●) DSC and (×) DMTA for infinite cure time at various isothermal temperatures, T_{cure}.

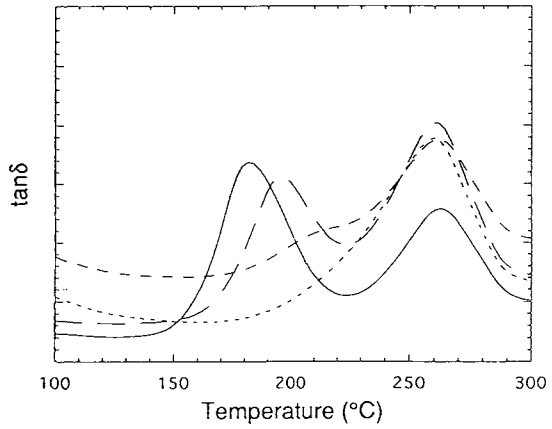

Figure 17 Tan δ spectra for rescans showing decreasing intensity of T_g for various cure temperatures: (——) 130°C; (— — —) 140°C; (- - - - -) 150°C; (----------) 160°C.

thus, the points should lie on a straight line of $y = x$. However, in the TGAP/DDS system, as in most others,[48] the points lie above this line. The reasons for this phenomenon are a combination of several factors: First, there is the effect due to the sample cure exotherm raising T_{cure} above that of the oven temperature as well as further curing due to thermally rescanning the sample. Another contribution causing T_g to be above T_{cure} would be the further reaction that is able to take place in the rigid three-dimensional network. Since the functionality of TGAP is very high, there is still likely to be reactive sites available even when they are locked into the network. Evidence of this is seen in the DMTA spectrum which shows that the modulus continues to increase for a short time after the vitrification (at which $T_g = T_{cure}$; by definition) peak in the tan δ spectrum. Another contribution to the increase is that the T_g is arbitrarily chosen to be the tan δ peak, whereas, in reality, the glass transition occurs over a range of temperatures.

During the DMTA rescan of a cured epoxy resin (after the first major T_g relaxation when the material is still rubbery), it can be seen to begin curing again, due to the high residual functionality. The material continues this extra cure until a final, ultimate T_g is reached (T_g^u). This is the highest T_g that is able to be achieved for this system and was found to be approximately 264°C. During the rescans of the isothermally cured material, it was found that with increasing temperature the intensity of the tan δ peak of the first T_g decreases with respect to the T_g^u peak until the 160°C cure sample, after which it is no longer visible. This means then that by curing TGAP/DDS at 170°C a material can be produced with a T_g of around 264°C. This phenomenon is shown in Figure 17. The intensity of the tan δ peak reflects the mobility of the network, and given the highly crosslinked nature of this network, it appears that the mobility at T_g is becoming less and less due to the increasing conversion, fewer reactive sites, and higher crosslink density. This phenomenon has been observed elsewhere[50] and was attributed to the coherence of the network.

Figure 18 shows the plot of T_g vs. conversion for various cure temperatures. It can be seen that the glass transition temperatures fall on the same curve, irrespective of the cure temperature, i.e., they are a function of degree of conversion only, which correlates with recent modeling by Wang and Gillham,[51] indicating that the cure mechanism is independent of temperature.

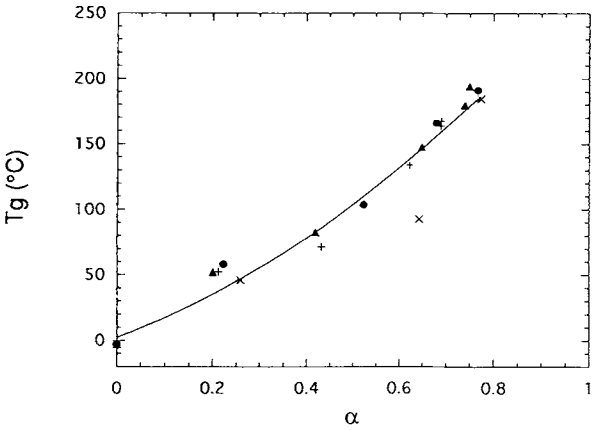

Figure 18 T_g as a function of conversion (α) for a range of isothermal cure temperatures: (+) 120°C; (▲) 140°C; (●) 160°C; (×) 180°C.

CONCLUSIONS

In this article, we have presented the kinetic and thermal details of the cure of a trifunctional epoxy resin, triglycidyl-*p*-aminophenol (TGAP) and diaminodiphenyl sulfone (DDS) using thermal analysis techniques. The data presented here are complementary to a near-infrared study of the same system presented elsewhere.[17]

Dynamic scanning and isothermal kinetic studies were undertaken and their relative merits discussed. DSC work indicated that essentially total thermal conversion ($\alpha = 0.99$) was possible with cure temperatures of 220°C. By assuming a general mathematical dependence of the reaction rate as a function of conversion, activation energies were determined as a function of degree of cure and compared to the variation of activation energy with difunctional and tetrafunctional epoxy systems. The dramatic increase of activation energy with conversion in the TGAP system was similar to that seen in the tightly crosslinked tetrafunctional system TGDDM, indicating a similar physicochemical reaction mechanism and network growth which, after gelation, leads to a rapid increase in chain rigidity and, in turn, influences the reaction kinetics.

Detailed isothermal studies indicated a relatively poor fit of TGAP polymerization kinetics to an autocatalytic model, particularly at high conversions which are greatly affected by the onset of diffusion control. The deviation from the fit occurred beyond about 50% conversion—effectively between gelation and vitrification. Two models were used to fit diffusion control—the model of Barton[22] which assumed a linear decrease in the reaction rate constant with conversion and that of Chern and Poehlein[45] who assumed a WLF-type dependence on reaction rate as vitrification dominates the free volume and molecular mobility of the reacting species. The Chern model proved very useful in determining conversion figures at which diffusion-control kinetics began to dominate.

Dynamic mechanical analysis was crucial in being able to link key polymerization events with the degree of conversion. It was shown that conversion at gelation was relatively cure temperature-independent, whereas indicators of higher conversion events such as vitrification were strongly cure temperature-dependent. The latter clearly reflected the greater degree of conversion necessary to cause immobility of the reactive groups upon vitrification as temperature was increased. In this work, it was found that for TGAP glass transitions for both DSC and DMTA at infinitely long cure times, T_g^u were significantly greater than was the isothermal cure temperature. The evolution of the T_g of the network was monitored at varying temperatures and indicated that the reaction does not completely cease until the modulus has plateaued. A TTT diagram was constructed which enables the cure profile to be altered to suit the desired final properties. Finally, the glass transition was found to be uniquely determined by degree of cure—irrespective of the isothermal temperature of cure.[52]

REFERENCES

1. A. J. Kinloch, in *Structural Adhesives*, A. J. Kinloch, Ed., Elsevier, London, 1986, Chap. 5.
2. J. L. Hendrick, I. Yilgor, G. L. Wilkes, and J. E. McGrath, *Polym. Bull.*, **13,** 201 (1985).
3. S. C. Kim and H. R. Brown, *J. Mater. Sci.*, **22,** 2589 (1987).
4. J. A. Cecere and J. E. McGrath, *Polym. Prepr.*, **27,** 299 (1986).
5. R. S. Raghava, *J. Polym. Sci. Polym. Phys. Ed.*, **26,** 65 (1988).
6. C. B. Bucknall and A. H. Gilbert, *Polymer*, **30,** 213 (1989).
7. K. S. Jagadeesh, Siddaramaiah, and V. J. Kalpagam, *J. Appl. Polym. Sci.*, **40,** 1281 (1990).
8. I. K. Partridge, in *Advanced Composites*, I. K. Partridge, Ed., Elsevier, London, UK, 1988, Chap. 1.
9. P. J. Pearce, R. G. Davidson, and C. E. M. Morris, *J. Appl. Polym. Sci.*, **27,** 4501 (1982).
10. C. B. Bucknall, *Composites*, **15,** 129 (1984).
11. C. B. Bucknall and I. Partridge, *Br. Polym. J.*, **15,** 71 (1983).
12. C. B. Bucknall and I. Partridge, *Polymer*, **24,** 639 (1983).
13. D. J. Hourston and J. M. Lane, *Polymer*, **33,** 1379 (1992).
14. J. L. Hedrick, I. Yilgor, M. Jurek, J. C. Hedrick, G. L. Wilkes, and J. E. McGrath, *Polymer*, **32,** 2020 (1991).
15. A. J. MacKinnon, S. D. Jenkins, P. T. McGrail, and R. A. Pethrick, *Macromolecules*, **25,** 3492 (1992).
16. A. J. MacKinnon, S. D. Jenkins, P. T. McGrail, and R. D. Pethrick, *Polymer*, **34,** 3252 (1993).
17. R. J. Varley, G. R. Heath, D. G. Hawthorne, J. H. Hodgkin, and G. P. Simon, *Polymer*, **36,** 1341 (1995).
18. C. J. De Bakker, N. A. St. John, and G. A. George, *Polymer*, **37,** 716 (1993).
19. A. Apicella, L. I. Nicolais, and P. Passerini, *J. Appl. Polym. Sci.*, 2083 (1984).
20. A. Apicella and L. I. Nicolais, *Adv. Polym. Sci.*, **72,** 69 (1985).
21. M. T. Aronhime and J. K. Gillham, *Adv. Polym. Sci.*, **78,** 83 (1986).
22. J. M. Barton, *Polymer*, **21,** 603 (1980).

23. H. Stutz and J. Mertes, *J. Polym. Sci. Part A Polym. Chem.*, **31,** 2031 (1983).
24. H. E. Kissinger, *Anal. Chem.*, **29,** 1702 (1957).
25. K. S. Jagadeesh and Siddarmaiah, *Polym. Int.*, **26,** 129 (1991).
26. J. M. Barton, *Adv. Polym. Sci.*, **72,** 111 (1985).
27. L. Chiao, *Macromolecules,* **23,** 1286 (1990).
28. K. C. Cole, J. H. Hechler, and D. Noel, *Macromolecules,* **27,** 3098 (1991).
29. K. Dusek, *Polym. Bull.*, **13,**, 321 (1985).
30. W. X. Zukas, N. S. Schneider, and W. J. MacKnight, *Polym. Mater. Sci. Eng.*, **49,** 588 (1983).
31. D. Greenfield, PhD Thesis, Brunel University, UK, 1988.
32. J. M. Barton, *Br. Polym. J.*, **18,** 1 (1986).
33. U. Khanna and M. Chanda, *J. Appl. Polym. Sci.*, **49,** 319 (1993).
34. K. Horie, H. Hiura, M. Sawada, I. Mita, and H. Kambe, *J. Polym. Sci. Part A-1,* **8,** 135 (1970).
35. N. S. Enikolopiyan, *Pure Appl. Chem.*, **48,** 317 (1976).
36. I. T. Smith, *Polymer,* **2,** 95 (1961).
37. J. S. Shim, W. Lee, and J. Jang, *Polym. J.*, **23,** 903 (1991).
38. J. S. Shim, W. Lee, and J. Jang, *Polym. J.*, **23,** 911 (1991).
39. J. Mijovic, J. Kim, and J. Salby, *J. Appl. Polym. Sci.*, **29,** 1449 (1984).
40. M. E. Ryan and A. Dutta, *Polymer,* **20,** 203 (1979).
41. S. Sourour and M. R. Kamal, *Thermochim. Acta,* **14,** 41 (1976).
42. N. A. St. John, G. A. George, P. A. Cole-Clarke, M. E. Mackay, and P. J. Halley, *High Perf. Plast.*, **5,** 21 (1993).
43. K. C. Cole, J. J. Hechler, and D. Noel, *Macromolecules,* **24,** 3098 (1991).
44. J. M. Kenny, *J. Appl. Sci.*, **51,** 765 (1994).
45. C. S. Chern and G. W. Poehlein, *Polym. Eng. Sci.*, **27,** 782 (1987).
46. K. C. Cole, *Macromolecules,* **24,** 3093 (1991).
47. P. J. Flory, *Principles of Polymer Chemistry,* Cornell University Press, Ithaca, NY, 1953.
48. K. Hofman and W. G. Glasser, *Thermochim. Acta,* **166,** 169 (1990).
49. J. B. Enns and J. K. Gillham, *J. Appl. Polym. Sci.*, **28,** 2567 (1983).
50. G. A. Senich, W. J. MacKnight, and N. S. Schneider, *Polym. Sci. Eng.*, **313,** 19 (1979).
51. X. Wang and J. K. Gillham, *J. Appl. Polym. Sci.*, **45,** 2127 (1992).
52. G. Wisanrakkit and J. K. Gillham, *J. Appl. Polym. Sci.*, **41,** 2885 (1990).

Received September 1, 1995
Accepted December 11, 1995